Journal of Solid State Chemistry 181 (2008) 2418–2423

Contents lists available at ScienceDirect

Journal of Solid State Chemistry

journal homepage: www.elsevier.com/locate/jssc

Role of crystallite size on the photoluminescence properties of $SrIn_2O_4:Eu^{3+}$ phosphor synthesized by different methods

N. Lakshminarasimhan *,[1], U.V. Varadaraju

Materials Science Research Centre and Department of Chemistry, Indian Institute of Technology Madras, Chennai 600 036, India

ARTICLE INFO

Article history:
Received 14 February 2008
Received in revised form
31 May 2008
Accepted 4 June 2008
Available online 6 June 2008

Keywords:
Photoluminescence
Eu^{3+}
$SrIn_2O_4$
Combustion synthesis
Crystallite size

ABSTRACT

Photoluminescence (PL) of Eu^{3+} was studied in $SrIn_2O_4$ host lattice. A complete solid solubility of Eu^{3+} has been found in the series $SrIn_{2-x}Eu_xO_4$ [$x = 0$–2.0]. The phase formation at a relatively low temperature and in a very short duration was achieved by combustion synthesis (CS). Concentration quenching of luminescence has been observed in $SrIn_{2-x}Eu_xO_4$ [$x = 0.1$–2.0] and the critical concentration for maximum emission was found to be with $x = 0.3$. In order to find the role of crystallite size on the PL properties of $SrIn_2O_4:Eu^{3+}$, the results obtained with phosphors synthesized by solid state reaction (SSR) and CS methods were compared.

1. Introduction

Recent developments in display technology have resulted in various advanced display devices such as electroluminescent (EL), alternating current thin film electroluminescent (ACTFEL), field emission (FEDs), plasma display panels (PDPs) and vacuum fluorescent displays (VFDs) [1]. One of the current research interests in the area of luminescent materials is the development of phosphors for low-voltage ($\leqslant 1$ kV) emissive flat-panel displays. In order to improve the characteristics of the phosphors for low-voltage applications, conventionally a conductive material such as In_2O_3 is added to the host materials as in the case of ZnS:Ag, Cl phosphor [2]. Among the indium-based oxides, $SrIn_2O_4$ is found to be an attractive host lattice for rare earth ions which is evident from the recent reports by different research groups [3–7]. The semiconducting $SrIn_2O_4$ and $CaIn_2O_4$ served as host lattice for Pr^{3+} and Tb^{3+} activators for red and green phosphors, respectively [3–5]. Enhancement in the efficiency of $SrIn_2O_4:Pr^{3+}$ phosphor has been achieved by doping Gd^{3+} or La^{3+} with control of the Sr^{2+} content [6]. The host-sensitized luminescence of Dy^{3+}, Pr^{3+} and Tb^{3+} has been observed in $SrIn_2O_4$:*RE* phosphors [7].

Eu^{3+} being a well-known red emitter, its photoluminescence (PL) properties in $SrIn_2O_4$ host lattice are of interest to investigate. Baszczuk et al. [8] investigated the PL of Eu^{3+} in $SrIn_2O_4$ and found that Eu ion substitutes both Sr and In positions in the crystal structure. More recently, the possibility of $SrIn_2O_4:Eu^{3+}$ phosphor for its application as a red phosphor in the white-light-emitting diodes for the solid-state lighting technology has been explored [9]. It is known that $SrIn_2O_4$ phase formation by solid state reaction (SSR) occurs by heating the precursor oxides for a long duration (24–36 h) at very high temperatures in the range between 1200 and 1400 °C [3,10]. Here we made an attempt to synthesize $SrIn_2O_4:Eu^{3+}$ phosphor in a short duration through a combustion synthesis (CS) method. The CS method basically involves the reaction between an oxidizer such as metal nitrates, ammonium nitrate and ammonium perchlorate and an organic fuel, typically urea, carbohydrazide or glycine. The reaction is highly exothermic. CS method has been mainly adopted to synthesize fine particles of aluminates and ferrites [11–15]. The process has later been extended to synthesize various inorganic compounds such as sodium zirconium phosphate (NZP) [14], tungstates [16], etc. Sometimes, CS process does not result in the desired product, instead, it leads to a highly sinteractive precursors which on further annealing form the desired final product [17,18]. The products obtained by CS are more homogeneous and have smaller particle size than those obtained by the conventional high temperature SSR method. CS of Eu^{3+}-doped Al_2O_3 has been reported and the phosphor exhibited a strong red emission due to $^5D_0 \rightarrow {}^7F_2$ transition of Eu^{3+} [19,20]. Recent review shows that the CS is a facile route to obtain rare earth doped fine particle lamp phosphors in a very short duration [21,22]. CS of MIn_2O_4:Tb (M = Ca and Sr) phosphors has been reported and very recently the $SrIn_2O_4:Eu^{3+}$ phosphor has been synthesized by CS method to study its usefulness as a red

* Corresponding author.
E-mail address: nlnsimha@gmail.com (N. Lakshminarasimhan).
[1] Present address: Postdoctoral Research Associate, School of Environmental Science and Engineering, Pohang University of Science and Technology (POSTECH), Pohang 790 784, South Korea.

0022-4596/$ - see front matter © 2008 Elsevier Inc. All rights reserved.
doi:10.1016/j.jssc.2008.06.005

phosphor for white-light-emitting diodes [9,23,24]. However, no comparison of PL properties of $SrIn_2O_4$:Eu^{3+} phosphor synthesized by conventional SSR and CS methods has been made. A comparison of PL properties of phosphors synthesized by different routes becomes essential to evaluate the suitability of synthesis method when the applications of phosphors are concerned. Here we report the PL properties of Eu^{3+} in the semiconducting oxide $SrIn_2O_4$ synthesized by high temperature SSR method and the comparison of the properties with the phosphor synthesized in a very short duration and at low temperature through CS method.

2. Experimental

2.1. Synthesis

2.1.1. Solid state reaction

The phosphor compositions of the formula $SrIn_{2-x}Eu_xO_4$ [$x = 0$–2.0] were synthesized by conventional high temperature SSR method. Stoichiometric amounts of $SrCO_3$ (Cerac, 99.99%), In_2O_3 (Cerac, 99.5%) and Eu_2O_3 (Indian Rare Earths, 99.9%) were thoroughly ground and heated at 550 °C for 12 h. The obtained powders were again ground, made into pellets and sintered at 1200 °C for 24 h.

2.1.2. Combustion synthesis

Two selected phosphor compositions, $SrIn_{1.9}Eu_{0.1}O_4$ and $SrIn_{1.7}Eu_{0.3}O_4$, were prepared by CS method. Stoichiometric amounts of In_2O_3 (Cerac, 99.5%) and Eu_2O_3 (Indian Rare Earths, 99.9%) were dissolved in boiling conc. HNO_3 to convert the oxides into nitrates. Stiochiometric amount of $SrCO_3$ (Cerac, 99.99%) was then added to the above nitrate mixture. The mixture taken in a glass beaker was stirred well to get a homogeneous clear solution. Urea was used as a fuel. The molar ratio of the reactants $Sr(NO_3)_2$:$In(NO_3)_3$:$Eu(NO_3)_3$:$(NH_2)_2CO$ is 1:1.9:0.1:6.667. After the addition of urea to the solution, a slurry was obtained. This slurry was directly introduced into a preheated muffle furnace at 550 °C. Within 5 min, the mixture started boiling and produced a flame that sustained for few seconds. The product was then air quenched to room temperature (RT). The combustion process resulted in a fine pale yellow powder. The powder was ground well and small portions of it were used for calcination at various temperatures to establish the phase formation temperature. The powders were introduced into a preheated muffle furnace kept at various temperatures, viz., 600, 700, 800 and 900 °C, held at this temperature for 1 h and then air quenched to RT.

2.2. Characterization

The synthesized phosphors were characterized by powder X-ray diffraction (XRD) for the phase purity using Cu-$K\alpha_1$ radiation (P3000, Rich Seifert). The lattice parameters were calculated by least-square fitting method. Particle morphology was analyzed by scanning electron microscopy (Philips XL 30S). Diffuse reflectance UV–Visible spectra were recorded using a UV–VIS spectrometer with an integrating sphere attachment (V-560, Jasco). $BaSO_4$ was used as reference. PL excitation and emission spectra were recorded at RT using a spectrofluorometer (FP-6500, Jasco). An R-60 glass filter was used near the emission slit while recording the excitation spectra ($\lambda_{em.} = 614$ nm) in order to eliminate the lower order reflections.

3. Results and discussion

3.1. Phase formation

The powder XRD patterns of select phosphor compositions in the series $SrIn_{2-x}Eu_xO_4$ [$x = 0$–2.0] synthesized by SSR method are shown in Fig. 1. From the diffraction patterns, it is clear that all the compositions are isostructural with the parent $SrIn_2O_4$ phase. $SrIn_2O_4$ crystallizes with an orthorhombic symmetry and has $CaFe_2O_4$-type crystal structure [25]. There are two In sites, In(1) and In(2), both having six coordination environment with small variations in the In–O bond lengths. The $In(1)O_6$ octahedron shares its edges with another $In(1)O_6$ octahedron forming a repeat unit and these units share corners with a similar unit formed by $In(2)O_6$ octahedra resulting in a zig-zag chain structure.

The reflections in the powder XRD patterns show a shift towards lower angles with increase in Eu^{3+} concentration revealing an increase in the lattice parameters. The calculated lattice parameters of $SrIn_{2-x}Eu_xO_4$ are listed in Table 1 and the variation with Eu content is shown in Fig. 2. The lattice parameter variation shows an increase in all three lattice parameters with increasing concentration of Eu^{3+} as expected based on the bigger

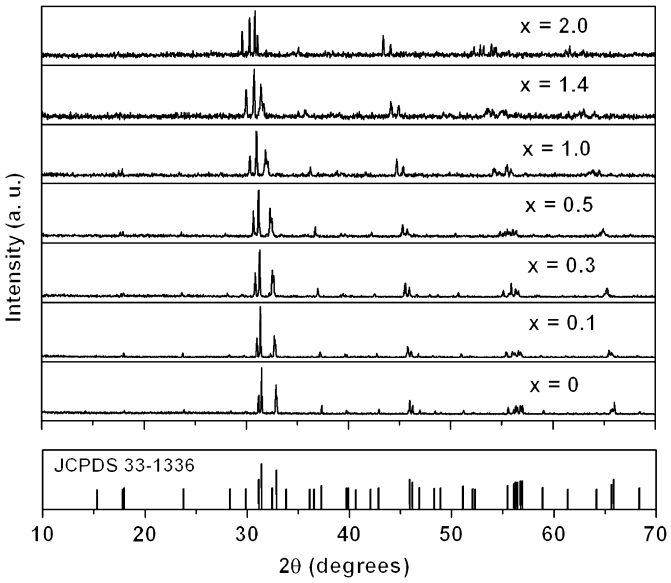

Fig. 1. Powder X-ray diffraction patterns of $SrIn_{2-x}Eu_xO_4$ synthesized by SSR method.

Table 1
Calculated lattice parameters of $SrIn_{2-x}Eu_xO_4$ [$x = 0$–2.0] synthesized by SSR method

X	a (Å)	b (Å)	c (Å)
0.0	9.8082	11.4578	3.2581
0.1	9.8390	11.5237	3.2721
0.2	9.8494	11.5403	3.2828
0.3	9.8598	11.5907	3.2939
0.4	9.8702	11.6076	3.3056
0.5	9.8806	11.6417	3.3183
0.6	9.8598	11.6589	3.3242
0.8	9.8806	11.7283	3.3459
1.0	9.9228	11.7811	3.3685
1.2	9.9762	11.8528	3.3819
1.4	9.9870	11.9073	3.4264
1.6	10.0305	11.9813	3.4686
1.8	10.0857	12.0377	3.4759
2.0	10.1419	12.0757	3.4929

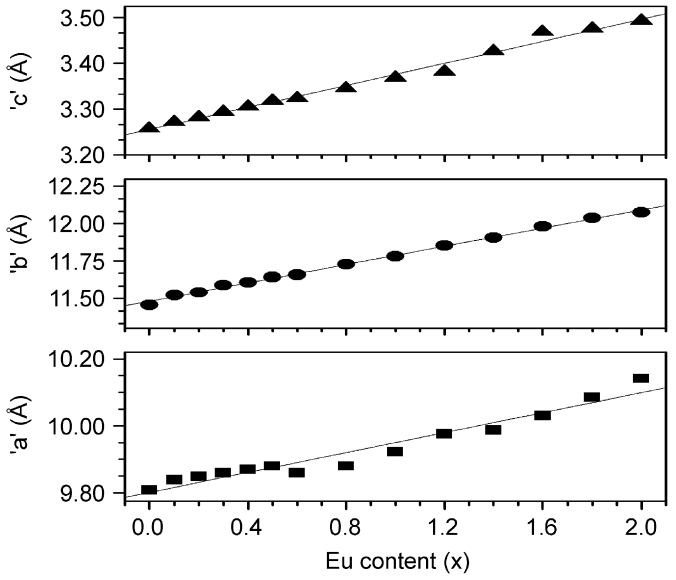

Fig. 2. Lattice parameters variation with Eu content in $SrIn_{2-x}Eu_xO_4$ [$x = 0$–2.0] synthesized by SSR method.

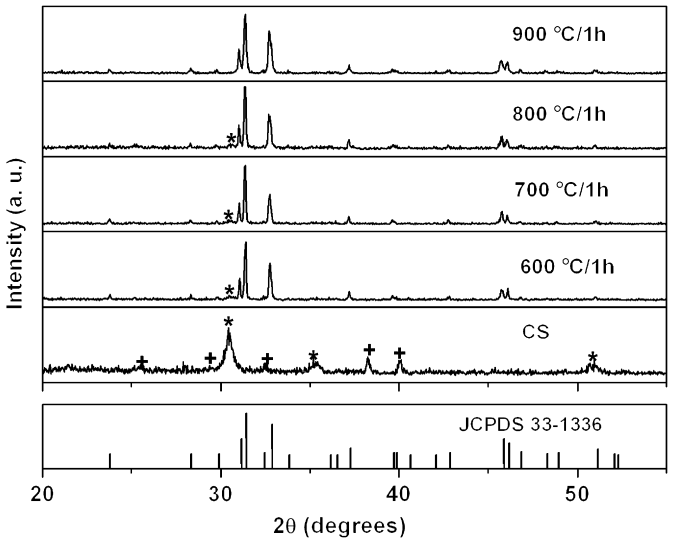

Fig. 3. Powder X-ray diffraction patterns of $SrIn_{1.9}Eu_{0.1}O_4$ by CS followed by calcination at different temperatures; (*) In_2O_3 and (+) $Sr(NO_3)_2$.

size of Eu^{3+} (0.95 Å) than In^{3+} (0.79 Å) [26]. A near linear variation in the lattice parameters reveals the existence of a complete solid solution in $SrIn_{2-x}Eu_xO_4$ and this is possible due to the fact that both the end members, $SrIn_2O_4$ and $SrEu_2O_4$, are isostructural compounds [27].

The powder XRD patterns of $SrIn_{1.9}Eu_{0.1}O_4$ obtained by CS and CS followed by calcination at different temperatures are shown in Fig. 3. The reported pattern of $SrIn_2O_4$ from JCPDS (File no. 33-1336) is also shown as a reference. The powder XRD pattern of the sample as obtained by CS method shows the absence of reflections corresponding to $SrIn_2O_4$ phase. The observed reflections were identified as due to In_2O_3 (marked with *) and unreacted $Sr(NO_3)_2$ (marked with +). CS method did not yield the desired product $SrIn_2O_4$, instead, it resulted in a highly reactive precursor In_2O_3 which is indicated by the broad reflections in the XRD pattern. This may be attributed to the low exothermicity of the combustion process which is not sufficient to complete the reaction [28]. Even in the case of $SrIn_2O_4$:Eu^{3+} phosphor synthesized by CS method, a final calcination at 1100 °C for 3 h has been used to obtain the phase [24]. Similar behavior was observed in the synthesis of Sr_2FeMoO_6 by CS method [18]. In the present study, the powder XRD pattern of the sample obtained after calcining the precursor at 600 °C for 1 h shows that the peaks are matching with the $SrIn_2O_4$ phase. This reveals that the phase formation could be achieved at such low temperature when compared to conventional SSR (1200 °C). However, an additional less intense line at $2\theta = 30.46°$ was observed and it has been identified as due to the unreacted In_2O_3. The unreacted In_2O_3 is present even in samples that were calcined at 700 and 800 °C. The powder XRD pattern of the sample obtained after calcining the precursor at 900 °C for 1 h showed no lines corresponding to unreacted In_2O_3 and all the lines were identified as due to $SrIn_2O_4$ phase. These results show the feasibility of synthesizing $SrIn_2O_4$ phase in a very short duration by CS followed by calcining the precursor at 900 °C for 1 h.

The powder XRD patterns of $SrIn_{1.9}Eu_{0.1}O_4$ synthesized by SSR and CS (followed by calcination at 900 °C) methods are shown in Fig. 4. The lines in the XRD pattern of the phosphor synthesized by CS are slightly broader than that of the phosphor synthesized by SSR method. The crystallite sizes of $SrIn_{1.9}Eu_{0.1}O_4$ obtained by both methods were calculated using the Scherrer formula [29]:

$$t = \frac{0.9\lambda}{B\cos\theta_B}$$

$$B = \sqrt{\left(B_M^2 - B_S^2\right)}$$

where λ is the wavelength of X-ray used (1.5406 Å), θ_B the Bragg angle, B is the line broadening (after correction due to instrumental broadening), B_M is the measured peak width in radians at half peak height of sample and B_S is the measured peak width in radians at half peak height of standard used (KCl). The crystallite size calculated for $SrIn_{1.9}Eu_{0.1}O_4$ synthesized by SSR is 1.2 μm and for the phosphor synthesized by CS is 0.6 μm. This result clearly shows that CS yielded a phosphor with smaller crystallite size compared to the phosphor synthesized by conventional SSR method. The scanning electron micrographs of $SrIn_{1.9}Eu_{0.1}O_4$ synthesized by SSR and CS methods are shown in Fig. 5. From these pictures, it is clear that the particle size of $SrIn_{1.9}Eu_{0.1}O_4$ synthesized by CS is lower than the phosphor synthesized by SSR

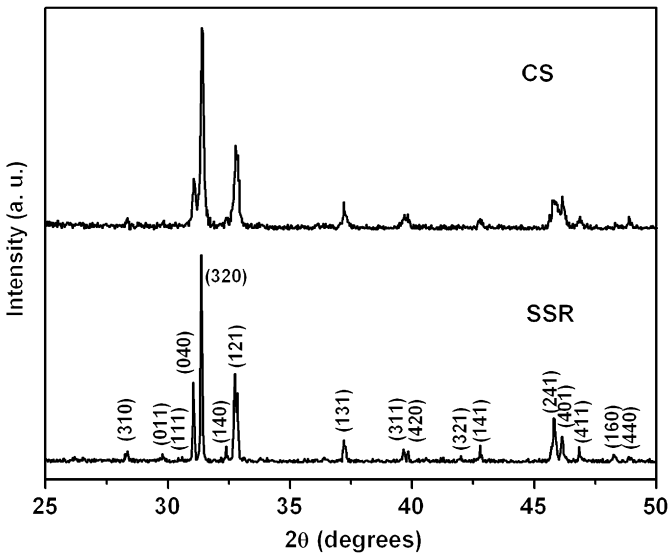

Fig. 4. Powder X-ray diffraction patterns of $SrIn_{1.9}Eu_{0.1}O_4$ synthesized by SSR and CS methods.

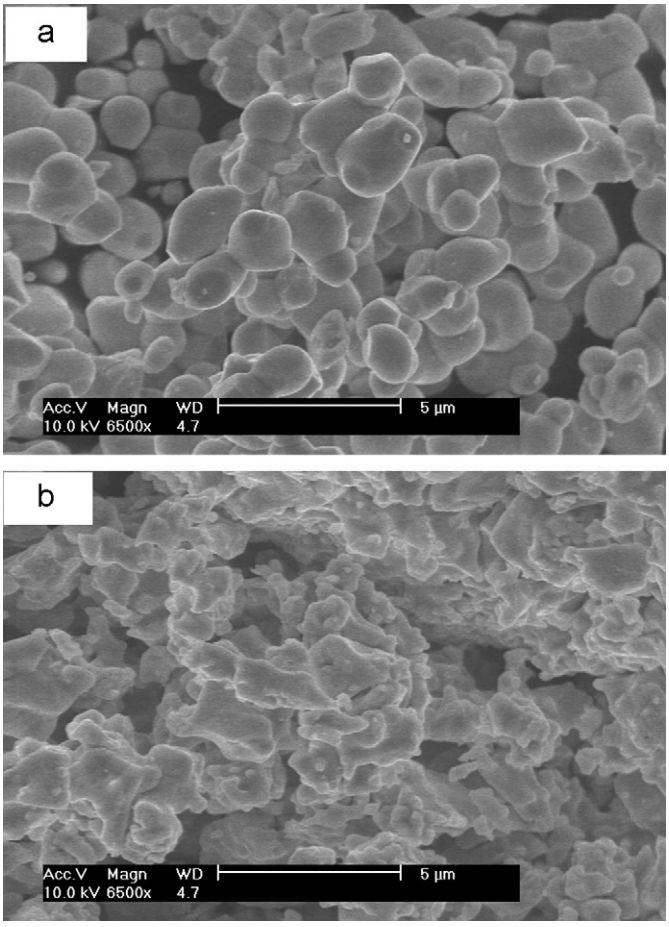

Fig. 5. Scanning electron micrographs of $SrIn_{1.9}Eu_{0.1}O_4$ synthesized by (a) SSR and (b) CS methods.

method. Notably the particles obtained by SSR method are more uniform in size with well-defined grain boundaries than the particles obtained by CS method. This reveals a high degree of agglomeration of the particles in the case of CS.

3.2. Diffuse reflectance UV– Visible spectroscopy

The optical absorption of the host $SrIn_2O_4$ and Eu-substituted phosphors were monitored by diffuse reflectance UV–Visible spectroscopy. The diffuse reflectance spectra of $SrIn_2O_4$, $SrEu_2O_4$ and $SrIn_{1.9}Eu_{0.1}O_4$ synthesized by SSR and CS methods are shown in Fig. 6. An absorption edge at around 450 nm with a maximum absorption at 320 nm are observed for $SrIn_2O_4$ and these values are in good agreement with the literature reports for $SrIn_2O_4$ [30,31]. From the reported electronic structure, it is understood that the optical transition occurs from the O 2*p* orbital to the hybridized In 5*s* and 5*p* orbitals, i.e., from the top of the valence band to the bottom of the conduction band [31,32]. In the case of $SrEu_2O_4$, more intense absorptions at 395 and 465 nm as shown clearly in the inset are due to $^7F_0 \rightarrow {}^5L_6$ and $^7F_0 \rightarrow {}^5D_2$ excitations, respectively. The absorption at around 260 nm is due to O^{2-} to Eu^{3+} charge transfer (c.t.) absorption.

3.3. Photoluminescence spectroscopy

3.3.1. $SrIn_{2-x}Eu_xO_4$ by solid state reaction

The PL excitation and emission spectra of $SrIn_{1.9}Eu_{0.1}O_4$ synthesized by SSR method are shown in Fig. 7. The excitation spectrum corresponding to the emission at 614 nm consists of

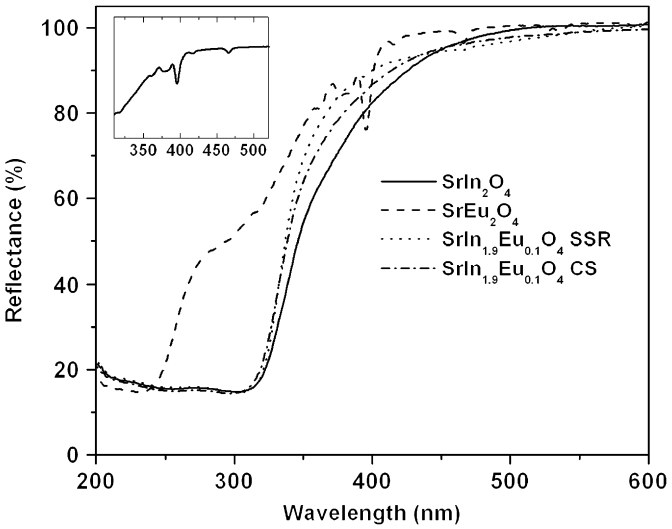

Fig. 6. Diffuse reflectance UV–Visible spectra of $SrIn_2O_4$, $SrEu_2O_4$, $SrIn_{1.9}Eu_{0.1}O_4$—SSR and $SrIn_{1.9}Eu_{0.1}O_4$—CS; The inset showing the spectrum of $SrEu_2O_4$.

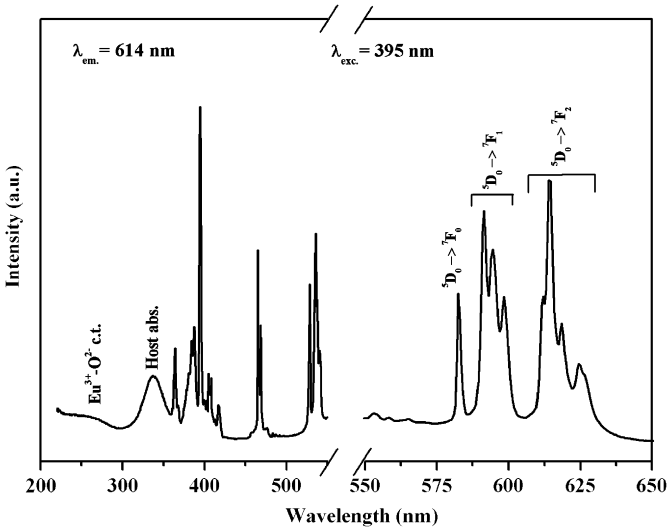

Fig. 7. Photoluminescence (a) excitation and (b) emission spectra of $SrIn_{1.9}Eu_{0.1}O_4$ synthesized by SSR method.

sharp absorption lines in the region 350–550 nm. These absorptions are due to excitation of Eu^{3+} from the ground $^7F_0$ state to various higher excited states. A weak band observed at 260 nm corresponds to the Eu^{3+}– O^{2-} c.t. band. These positions are in good agreement with the absorptions observed in the diffuse reflectance UV–Visible spectrum. A broad band at 337 nm is observed in the excitation spectrum. Baszczuk et al. [8] identified a similar band at 325 nm in $SrIn_2O_4$:Eu^{3+} and assigned it as $^7F_0 \rightarrow 4f^{n-1}5d^2$ transition of Eu^{2+} ion which could have formed by substitution of Eu^{3+} ion at Sr site. It has been reported that in the case of $CaIn_2O_4$:Tb^{3+} the band observed in the excitation spectrum at 318 nm is due to the host lattice absorption [5]. Similarly, the absorption band at 337 nm in the present study can be attributed to the host lattice absorption since the host $SrIn_2O_4$ is a semiconductor with band gap energy of 3.6 eV [4]. Also, the presence of the host absorption band in the excitation spectrum of Eu^{3+} shows the possibility of host to Eu^{3+} energy transfer [33]. Recently, it has been reported that host-sensitized luminescence occurs in $SrIn_2O_4$ doped with Dy^{3+}, Pr^{3+} and Tb^{3+} ions [7]. $SrIn_2O_4$

exhibits a broad absorption band in the region 297–302 nm in rare earth doped compositions. The energy transfer from the host $SrIn_2O_4$ to the rare earth dopant is complete for Pr^{3+} and Tb^{3+} and it is incomplete for Dy^{3+}. All these reports confirm our assignment of the band at 337 nm to the host lattice absorption in $SrIn_2O_4$:Eu^{3+} phosphor. However, in the present study no enhancement of Eu^{3+} emission intensity was observed when the excitation was 337 nm (host). The reason for this may be the higher concentration of Eu^{3+} used in the present study when compared with the concentration of rare earth ions used in the study by Liu et al. [7].

The emission spectrum of $SrIn_{1.9}Eu_{0.1}O_4$ under 395 nm excitation consists of very sharp lines with clear splittings in the region 550–670 nm due to Eu^{3+}. The emission line at 582 nm is due to the $^5D_0 \rightarrow {}^7F_0$ transition and this is in good agreement with the results of Baszczuk et al. [8] and Taibi et al. [34] who studied the luminescence of Eu^{3+} in $SrRE_2O_4$ (RE = Eu, Gd, Y and In). Taibi et al. observed two emission lines corresponding to $^5D_0 \rightarrow {}^7F_0$ transition of Eu^{3+} in $SrRE_2O_4$ (RE = Gd, Y and In) by site selective excitation of this level at 77 K and attributed to the presence of Eu^{3+} in two different sites, I and II, in the crystal structure. The difference in energy between the two emission lines of $^5D_0 \rightarrow {}^7F_0$ transition observed were 12, 38 and 56 cm^{-1} in $SrIn_2O_4$, SrY_2O_4 and $SrGd_2O_4$, respectively. However, in the present study, we observed a single emission line corresponding to $^5D_0 \rightarrow {}^7F_0$ transition of Eu^{3+} in $SrIn_2O_4$. According to Taibi et al. [34], the difference between the two emission lines of $^5D_0 \rightarrow {}^7F_0$ transition depends on the size of the host lattice cations. As the size becomes smaller, the difference in the energy between the two emission lines of $^5D_0 \rightarrow {}^7F_0$ transition is less as observed in $SrIn_2O_4$:Eu^{3+}. It was also pointed out that with the host cation size of 0.76 Å the two sites, I and II, become equivalent and this is the reason for the observed smaller difference in energy (12 cm^{-1}) between the emission lines of $^5D_0 \rightarrow {}^7F_0$ transition in $SrIn_2O_4$:Eu^{3+} than in $SrRE_2O_4$:Eu^{3+} [RE = Gd and Y]. Since our measurements were made at RT and also the host cation is In^{3+}, we could not observe the difference in the emission lines of $^5D_0 \rightarrow {}^7F_0$ transition. In the emission spectrum, the lines observed in the region between 588 and 600 nm are due to the magnetic-dipole $^5D_0 \rightarrow {}^7F_1$ transition. The emission lines observed between 605 and 630 nm with a maximum at 614 nm correspond to the electric-dipole $^5D_0 \rightarrow {}^7F_2$ transition.

3.3.2. Concentration quenching

In order to find the role of concentration on the PL emission intensity of Eu^{3+} in the solid solution $SrIn_{2-x}Eu_xO_4$, the PL was recorded with higher Eu^{3+}-containing compositions. The variation in the emission intensity with Eu^{3+} content is followed by monitoring the emission intensity at 614 nm. The integrated area was measured. The variation in the intensity of $^5D_0 \rightarrow {}^7F_2$ transition with Eu^{3+} content is plotted in Fig. 8. The emission intensity of $^5D_0 \rightarrow {}^7F_2$ transition increased with increase in Eu^{3+} content from 0.1 to 0.3 and then decreased with further increase in Eu^{3+} content. The phosphor $SrIn_{1.7}Eu_{0.3}O_4$, when exposed to UV lamp, exhibited a relatively bright red emission among the other phosphors investigated in the present study. With increasing Eu^{3+} concentration, the distance between Eu^{3+} ions becomes less and this results in the migration of excitation energy among Eu^{3+} ions leading to quenching of the emission. Since the optical transitions of Eu^{3+} are forbidden, the energy migration can occur by exchange interaction [33]. The critical concentration of Eu^{3+} in $SrIn_{2-x}Eu_xO_4$ is at $x = 0.3$ beyond which the concentration quenching occurs.

3.3.3. Solid state reaction vs. combustion synthesis

The PL excitation and emission spectra of $SrIn_{1.9}Eu_{0.1}O_4$ and $SrIn_{1.7}Eu_{0.3}O_4$ synthesized by SSR and CS methods are shown in Fig. 9. There are no differences observed in the positions and

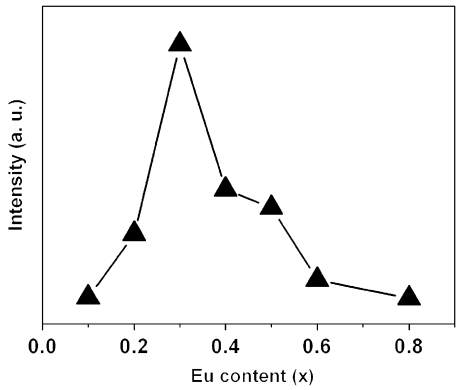

Fig. 8. Variation in photoluminescence emission intensity with concentration of Eu in $SrIn_{2-x}Eu_xO_4$ synthesized by SSR method.

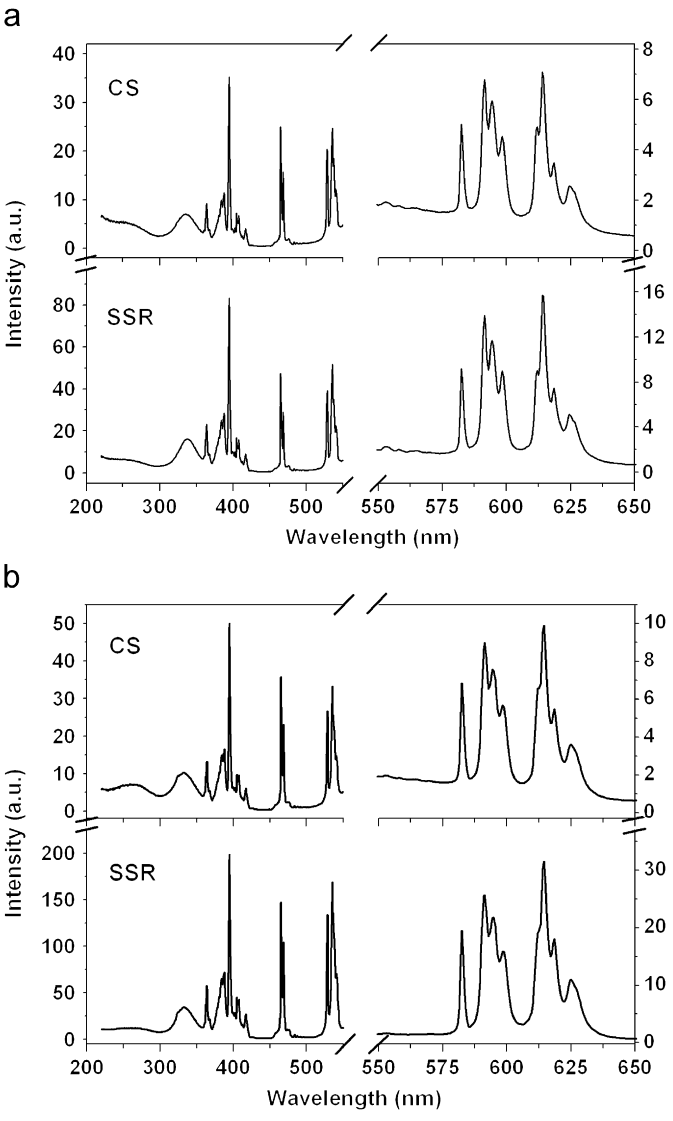

Fig. 9. Photoluminescence excitation and emission spectra of (a) $SrIn_{1.9}Eu_{0.1}O_4$ and (b) $SrIn_{1.7}Eu_{0.3}O_4$ synthesized by SSR and CS methods: $\lambda_{exc.} = 395$ nm and $\lambda_{em.} = 614$ nm.

features of the excitation and emission lines of Eu^{3+} in phosphors synthesized by both methods. However, in both compositions ($x = 0.1$ and 0.3), the intensities of excitation and emission lines of phosphors synthesized by SSR method are remarkably higher by

nearly twice than that of the phosphors synthesized by CS method. A strong dependence of the luminescence of a phosphor on its crystallite size is evident by the reports made by various research groups. Shea et al. [35] showed that the low-voltage cathodoluminescene efficiency of Y_2O_3:Eu^{3+} phosphor prepared by CS depends on the crystallite size and independent of the particle size. With smaller crystallites, the probability for non-radiative recombination becomes higher due to the increased number of atoms in the grain boundaries and on the surface, when compared to particles with larger crystallite size. The PL emission intensity of Y_2O_3:Eu^{3+} synthesized by spray pyrolysis method using organic additives exhibited a linear relation with the crystallite size and a high PL emission intensity was observed for larger crystallite size [36]. In another report, the PL intensities and quantum efficiencies of Y_2O_3:Eu^{3+} phosphor were higher with increased crystallite and particle sizes and in particular, the effect of crystallite size is predominant than the particle size effect [37]. In the case of Gd_2O_3:Eu^{3+} prepared by CS followed by annealing at 600, 700 and 800 °C, a higher PL excitation and emission intensities were observed for the phosphor annealed at 800 °C [38]. The reason for such behavior has been attributed to the large particles with better crystallization and also the high temperature calcination removes the defect centers which otherwise will act as non-radiative relaxation centers. In the present study, the crystallite size of $SrIn_2O_4$:Eu^{3+} synthesized by CS is lower than that of the phosphor synthesized by SSR method. Thus, the smaller crystallites with large agglomeration at grain boundaries of $SrIn_2O_4$:Eu^{3+} phosphor prepared by CS method results in the lower PL excitation and emission intensities. Although the CS produced $SrIn_2O_4$:Eu^{3+} phosphor in a short duration and at a relatively low temperature, improvement in the PL properties could not be realized. Our results clearly indicate the importance of the larger crystallite size of phosphors for improved PL properties as observed in the case of various phosphors and $SrIn_2O_4$:Eu^{3+} is not an exception to this observation.

4. Conclusions

Photoluminescence of Eu^{3+} in $SrIn_2O_4$ has been studied. A rapid synthesis of $SrIn_2O_4$:Eu^{3+} was achieved by CS method. The results showed that the single-phase formation is possible by heating the precursor obtained by CS at a relatively low temperature (900 °C vs. 1200 °C in SSR) for a short duration of 1 h. Increase in Eu^{3+} concentration resulted in the concentration quenching of the emission and the critical concentration was found with $x = 0.3$ in $SrIn_{2-x}Eu_xO_4$. The comparison of PL results of $SrIn_{2-x}Eu_xO_4$ [$x = 0.1$ and 0.3] synthesized by SSR and CS methods revealed a higher PL intensities for phosphors synthesized by SSR method and this is due to the larger crystallite size. An optimization of crystallite size for the improved PL properties of phosphors is essential when low temperature synthesis methods are being attempted.

Acknowledgments

The author N. Lakshminarasimhan acknowledges the Council of Scientific and Industrial Research, New Delhi for a research fellowship. The help rendered by Mrs. S. Srividya in the XRD measurements is kindly acknowledged.

References

[1] L.E. Shea, J. Electrochem. Soc. Interface 7 (1998) 24–27.
[2] S.W. Kang, B.S. Jeon, J.S. Yoo, J.D. Lee, J. Vac. Sci. Technol. B 15 (1997) 520–523.
[3] F.S. Kao, T.M. Chen, J. Solid State Chem. 155 (2000) 441–446.
[4] F.S. Kao, T.M. Chen, J. Solid State Chem. 156 (2001) 84–87.
[5] F.S. Kao, T.M. Chen, J. Lumin. 96 (2002) 261–267.
[6] H. Yamamoto, M. Abe, M. Ogura, S. Mitsumine, K. Uheda, S. Okamoto, J. Electrochem. Soc. 154 (2007) J15–J20.
[7] X. Liu, C. Lin, Y. Luo, J. Lin, J. Electrochem. Soc. 154 (2007) J21–J27.
[8] A. Baszczuk, M. Jasiorski, M. Nyk, J. Hanuza, M. Mączka, W. Stręk, J. Alloys Compd. 394 (2005) 88–92.
[9] C.E.R. García, N.P. López, G.A. Hirata, S.P. DenBaars, J. Phys. D: Appl. Phys. 41 (2008), 092005:1–092005:4.
[10] F.R. Cruickshank, D. McK. Taylor, F.P. Glasser, J. Inorg. Nucl. Chem. 26 (1964) 937–941.
[11] J.J. Kingsley, K. Suresh, K.C. Patil, J. Mater. Sci. 25 (1990) 1305–1312.
[12] J.J. Kingsley, N. Manickam, K.C. Patil, Bull. Mater. Sci. 13 (1990) 179–189.
[13] S. Castro, M. Gayoso, C. Rodríguez, J. Solid State Chem. 134 (1997) 227–231.
[14] E. Breval, D.K. Agrawal, J. Am. Ceram. Soc. 81 (1998) 1729–1735.
[15] J. McKittrick, L.E. Shea, C.F. Bacalski, E.J. Bosze, Displays 19 (1999) 169–172.
[16] U. Kameswari, A.W. Sleight, J.S.O. Evans, Int. J. Inorg. Mater. 2 (2000) 333–337.
[17] S. Sundar Manoharan, K.C. Patil, J. Solid State Chem. 102 (1993) 267–276.
[18] M. Venkatesan, U.V. Varadaraju, A.P. Douvalis, C.B. Fitzgerald, F.M.F. Rhen, J.M.D. Coey, J. Mater. Chem. 12 (2002) 2184–2186.
[19] N. Rakov, F.E. Ramos, G. Hirata, M. Xia, Appl. Phys. Lett. 83 (2003) 272–274.
[20] O. Ozuna, G.A. Hirata, J. McKittirck, Appl. Phys. Lett. 84 (2004) 1296–1298.
[21] S. Ekambaram, K.C. Patil, M. Maaza, J. Alloys Compd. 393 (2005) 81–92.
[22] S. Ekambaram, M. Maaza, J. Alloys Compd. 395 (2005) 132–134.
[23] S.P. Khatkar, V.B. Taxak, S.D. Han, J.-Y. Park, D. Kumar, Mater. Chem. Phys. 98 (2006) 528–531.
[24] Z. Yang, J. Tian, S. Wang, G. Yang, X. Li, P. Li, Mater. Lett. 62 (2008) 1369–1371.
[25] V.R.V. Schenck, Hk. Müller-Buschbaum, Z. Anorg. Allg. Chem. 398 (1973) 24–30.
[26] R.D. Shannon, C.T. Prewitt, Acta Crystallogr. B 25 (1969) 925–945.
[27] Hk. Müller-Buschbaum, J. Alloys Compd. 349 (2003) 49–104.
[28] R. Gopi Chandran, K.C. Patil, Mater. Lett. 10 (1990) 291–295.
[29] A.R. West, Solid State Chemistry and its Applications, Wiley, Singapore, 1989, pp. 174.
[30] J. Sato, N. Saito, H. Nishiyama, Y. Inoue, J. Phys. Chem. B 105 (2001) 6061–6063.
[31] J. Tang, Z. Zou, M. Katagiri, T. Kako, J. Ye, Catal. Today 93–95 (2004) 885–889.
[32] J. Sato, H. Kobayashi, Y. Inoue, J. Phys. Chem. B 107 (2003) 7970–7975.
[33] G. Blasse, B.C. Grabmaier, Luminescent Materials, Springer, Berlin, 1994.
[34] M. Taibi, E.A. Fidancev, J. Aride, M.L. Blaise, P. Porcher, J. Phys.: Condens. Matter 5 (1993) 5201–5208.
[35] L.E. Shea, J. McKittrick, M.L.F. Philips, J. Electrochem. Soc. 145 (1998) 3165–3170.
[36] K.Y. Jung, C.H. Lee, Y.C. Kang, Mater. Lett. 59 (2005) 2451–2456.
[37] W.-N. Wang, W. Widiyastuti, T. Ogi, I.W. Lenggoro, K. Okuyama, Chem. Mater. 19 (2007) 1723–1730.
[38] Y. Li, G. Hong, J. Lumin. 124 (2007) 297–301.